ICRF Heating in Alcator C-Mod: Present Status and Future Prospects*

M. Porkolab, C. Fiore, M. Greenwald,

J.C. Hosea[a], A. Hubbard, I. Hutchinson, J. Irby, E. Nelson-Melby,

E. Marmar, C.K. Phillips[a], J. Reardon, J. Rice, G. Schilling[a],

J. Terry, S. Wolfe, S. Wukitch, J.R. Wilson[a], and the Alcator Team

MIT Plasma Science and Fusion Center, Cambridge, MA 02139, USA

[a]*Princeton Plasma Physics Laboratory, Princeton, NJ, 08543, USA*

Abstract. Alcator C-Mod, the high field, high density, diverted, compact tokamak in the world's portfolio of high performance plasma fusion devices, is heated exclusively with ICRF auxiliary power. In this paper an overview of recent results is summarized, with particular attention given to the importance of RF operation and the flexibility afforded by different heating scenarios. Besides the routine minority heating operation, results in the mode conversion heating regime are also presented (mainly direct electron heating through mode converted ion Bernstein waves). Recent attempts at improving plasma performance by establishing internal transport barriers (ITBs) by various transient profile control techniques (the so-called Advanced Tokamak mode of operation) are also presented. Future improvements in performance afforded by the recent addition of a new 4-strap antenna and 4 MW of tunable (40-80 MHz) ICRF power are also discussed. Mode-conversion current drive (MCCD) and fast wave current drive (FWCD) will be among the many new options that will be tested with the goal of improving plasma performance.

INTRODUCTION

The primary auxiliary heating power in Alcator C-Mod has been provided by the 4.0 MW ICRF heating system operating at 80 MHz in D(H), D(^{3}He) or ^{3}He(H) plasmas [1-5]. This frequency corresponds to on-axis minority fundamental cyclotron resonance of protons at 5.3 T, and ^{3}He at 7.9 T in a dominantly deuterium plasma. In addition, mode-conversion heating in various combinations of the above listed ion species has also been tested [6]. To date up to 3.5 MW of RF power at 80 MHz has been injected by two pairs of poloidal strap antennas, driven 180 degrees out of phase between adjacent straps (dipole phasing) [7]. The two antennas are installed in adjacent ports. The current straps and the antenna housing boxes are plated with copper, and are protected by slanted Faraday shield rods which are coated with TiCN and B_4N. Each of these antennas is capable of withstanding 50 kV, and has been operated in both vacuum and plasmas at 40 kV at the full power capability (10 MW/m^2). The antennas are

driven by external resonant loops. The power spectrum peaks at $N_\parallel=10$ in vacuum. Typical loading resistances in plasma are in the 3-10 Ohm range for each antenna. In principle, the present set of antenna straps can be phased 90 degrees relative to each other for current drive experiments. However, the phase velocity would be higher than typical electron thermal speeds, hence single pass absorption would be rather low for fast wave current drive applications. The newly installed 4-strap PPPL antenna, to be described later, will launch lower phase velocity waves. This antenna is suitable for fast wave current drive experiments with electrons preheated by the MIT two strap antennas.

MINORITY HEATING RESULTS

Absorbing fast waves by hydrogen minority species in a deuterium plasma can be very efficient (typical single pass absorption in C-Mod is 80-90% for minority concentrations of 5-10%). Typical minority heating results at 5.3 T using the D(H) minority case are shown in Figs. 1-3. In Fig. 1 heating results from a high-power L-mode plasma shot [2], in Fig. 2 from an Elm-free H-mode shot [3], and in Fig. 3 from an "enhanced D-alpha" shot [4] are shown, respectively. It is seen that in this particular L-mode shot (before boronization) at a line average density of $1.0 \times 10^{20} \mathrm{m}^{-3}$, peak electron and ion temperatures of 4.0 keV are achieved with 3.5 MW of RF power at a plasma current of 0.8 MA. Similar results have been obtained even when RF power is applied during current ramping experiments in the early discharge evolution phase [8]. Note that due to low density the stored energy is only of order 100 kJ, and β_N values remain below 1.0. In contrast, in the ELM-free H-mode shot the density rises to $3.0 \times 10^{20} \mathrm{m}^{-3}$, the stored energy approaches 200 kJ, and β_N achieves a value of 1.5. Maximum H-factors of 2.4 have been obtained (relative to ITER-89 L-mode scaling) [9]. However, as may be seen in Fig. 2, as the discharge evolves the radiated power fraction increases dramatically due to the near-perfect particle (i.e., impurity) confinement while the energy confinement deteriorates and after about 0.5 sec the discharge collapses due to the excessive radiated power losses. By operating at relatively high neutral pressures and triangularity, the so-called "enhanced D-alpha" regime of operation is achieved [4,10,11] in which quasi-steady state conditions are obtained (Fig. 3). In this case the confinement achieves a value of 2.0 times ITER-89 L mode scaling, the stored energy reaches 200 kJ with a β_N of 1.5 as before, and the radiated power fraction remains around 25% even in the presence of high-power (3.0 MW) ICRF heating. It may be seen that the D-alpha emission increases significantly. The plasma current in these discharges is again 0.8 MA at a magnetic field of 5.4 T.

Minority heating at 80 MHz and 7.9 T in a deuterium majority plasma is achieved with the ^{3}He minority resonance (on-axis) [4,5]. Single pass absorption with ^{3}He minority ions in deuterium in C-Mod is only in the range of 10–15%, depending on plasma parameters. This is a consequence of the reduced left hand polarization of the fast wave for frequencies only 33% above the deuterium cyclotron

frequency [12]. Nevertheless, using a break-in-slope analysis technique of the stored energy, an overall absorption efficiency of 80% has been determined for minority concentrations of 3-4%. A typical shot is shown in Fig. 4. We see that the available power in this case is marginal relative to the H-mod threshold, and that ELM-free H-mode is achieved only after a relatively long "dithering" phase (see the D-alpha signal) when the plasma alternates back and forth between L-mode and H-mode regimes. In this discharge the peak values of T_e and T_i are near 3.0 keV at a line average electron density of $3.0 \times 10^{20} \mathrm{m}^{-3}$. The RF power in this case was only 2.5 MW. In general, it has been found that the available power (up to 3.5 MW net) is not sufficient to achieve good H-mode confinement in a reliable manner at 7.9 Tesla. Therefore, operation at 7.9 T has been limited and better results will depend on the successful commissioning of the new PPPL antenna and the additional 3 MW of ICRF power. The dependence of RF absorption efficiency on ^{3}He concentration is shown in Fig. 5.

During magnetic field scans it has been found that in L-mode the heating efficiency deteriorates rapidly as the resonance layer is moved off-axis (and in particular as the resonance layer is moved outside of the $q = 1$ surface). On the contrary, in H-mode the heating efficiency remains high, at least for $r/a \sim 0.5$ even when the minority resonance layer is located outside the $q = 1$ surface. It is believed that the H-mode thermal barrier near the edge prevents the rapid loss of energy and minority tail inside the transport barrier. This result is important since it will provide additional flexibility in future heating experiments with limited transmitter frequency availability and tuning capability.

TOROIDAL PLASMA ROTATION IN RF HEATED DISCHARGES

An important recent result in ICRF heated C-Mod plasmas has been the observation of significant toroidal rotation of impurity ions, such as argon or molybdenum. The rotation is deduced from the Doppler shifts of particular x-ray lines of these ions, and analysis indicates that the bulk plasma also rotates with comparable speeds [13,14]. A typical result is shown in Fig. 6 by the solid curves, corresponding to H-mode confinement. We see that upon application of 2.5 MW of RF power applied at 5.3 T (H minority heating with the resonance located on the plasma axis) significant toroidal rotation is observed, with the maximum speed approaching 100 km/sec. This plasma entered the H-mode confinement state, with significant increases in the stored energy, density and ion temperature, with the D_α line dropping suddenly and then rising, characteristic of the "enhanced" D_α H-mode regime in Alcator C-Mod [4,10,11]. We should also take note, however, of the dash-dotted lines, which correspond to nearly similar RF power and initial plasma parameters, but somewhat different triangularity and neutral gas pressure. This plasma did not enter the H-mode regime, and also, it did not achieve the large plasma rotation; in fact, the initial counter rotation was

brought to a stop and the plasma is nearly at rest. The increment in rotation has been found to be correlated to the change in stored energy. At the same time the confinement remained in L-mode, with significantly lower density than the H-mode case (almost half of the H-mode value). Nevertheless, the ion and electron temperatures increased substantially (in this figure only the ion temperature is shown), and confinement is in good agreement with L-mode scaling, verifying excellent RF absorption at the plasma center. This result is possibly in disagreement with the recently proposed theoretical model of plasma rotation caused by the drift of energetic ions [15]. It seems that in the L-mode case, the density being only about half that of H mode, the ions should assume significantly larger energies than those in H-mode where the collisional drag on ions is greatly enhanced and therefore the quasi-linear diffusion is less effective. As shown in Refs. [13,14], the rotation is nearly independent of the magnetic field (tested at two values, namely at $B = 5.3$ T and $B = 7.9$ T). As shown in Fig. 7, the rotation is not to the radial location of the resonance, for the range $r/a = 0 - 0.7$, as long as the plasma remains in H-mode. It was shown recently [13] that the rotation peaks on axis. The rotation speed is inversely proportional to I_p. The usual neoclassical mechanism of toroidal rotation based on the pressure gradient term does not contribute in any meaningful way to plasma rotation at the plasma center in the present experiments. Also, direct momentum input from RF waves is negligible, and there are no neutral beam sources in C-Mod plasmas. The dependance of the stored energy and toroidal rotation on minority concentration is shown in Fig. 8. We see that both the rotation speed and the stored energy decrease as the minority concentration increases above 10%. This result is not surprising since at these higher concentration ratios mode conversion begins to dominate with less efficient overall power absorption. Apparently the toroidal rotation is strongly coupled to the stored energy increase. Finally, perhaps the most surprising result to date is that recently significant co-rotation has been discovered even in Ohmically heated plasmas as long as Ohmic H-modes were produced by lowering the magnetic field and plasma current [13]. This result casts further doubt on the interpretation of rotation in the RF heated C-Mod plasmas as having to do with large minority ion orbits [15]. Further experimental tests are required to resolve this important issue.

POWER DEPOSITION BY MODE-CONVERSION

Heating by mode-converted ion Bernstein Waves (IBW) offers another way to heat plasmas, with the possibility of high single pass absorption and localized heating. Another application of this technique is profile control by driving currents on or off-axis, thus controlling the q-profile. Initial results in C-Mod were reported in Refs. [5,6]. In Fig. 9 we show a typical result where the power deposition profile was measured by modulating the RF power (1.2 MW in L-mode plasmas) while the electron temperature was determined by ECE measurements using the grating polychromator. The "break-in-slope" technique was used to

measure the instantaneous power deposition and its radial location was determined from different chords of the polychromator. Recently the deposition profile was modeled by the "TORIC" code (solid curve) and reasonably good agreement between theory and experiment was obtained. About 91% of the power is predicted to be deposited by the code, somewhat above the measured integrated value of 79%. The centrally peaked RF power deposition exceeds the Ohmic power density by about a factor of ten.

Off-axis power deposition profiles were also measured using ^{3}He minority species in a Deuterium plasma. Experimental results at 1.2 MA at a density of 2.5×10^{20}m^{-3} are shown in Fig. 10. Theoretical predictions of the mode conversion layer for a 22% minority species concentration at 7.9 T are also shown in Fig. 10. Owing to the coarse radial chord spacing (about 2 cm) of the polychromator, these results are more uncertain (see lack of data between $r/a = 0.35$ and 0.45) than the central absorption case. The deposited integrated RF power in this case is in the range 40-50% of the injected RF power (about 2.5 MW). More accurate results are expected in the coming campaign using a new ECE diagnostic with improved radial resolution.

Power absorption by electrons as a function of minority concentration is shown in Fig. 11 [16]. Absorption at concentrations below 5% is presumably dominated by minority absorption, resulting in ion heating (not monitored self-consistently in the present series of experiments). Absorption above 5% should be dominated by mode conversion resulting in direct electron heating (which is what is measured by the break in slope analysis). We see that experimentally power absorption on electrons of the order of 40-50% is obtained at concentrations above 15-20%, with considerable scatter. Modeling these results with the TORIC full wave code gives fair agreement with the data, if we assume a minority tail temperature that scales inversely with ^{3}He concentration. (It should be noted that the mode conversion package in TORIC has been improved since these calculations were performed and further data analysis is being carried out.)

RF TRANSMISSION EXPERIMENTS

A novel way of measuring single pass RF absorption was attempted by measuring the relative value of RF transmission, using 8 loop probes installed behind the inner wall tiles, opposite to one of the two RF antennas [17]. As the minority concentration is increased from shot to shot, the transmission factor decreases (see Fig. 12). The minority concentration ratio was measured by a neutral particle charge exchange diagnostic. The vertical axis corresponds to power received by the loop probe antennae, divided by P_{RF}, scaled to fit the prediction of the full-wave code FELICE [18], run with outward radiative boundary conditions. We see that the full wave code, which includes multiple reflections on the low field side, is in reasonable agreement with experiments if we assume that a fixed fraction of the power is lost by toroidal convection, etc. On the contrary, the

single pass theory ignoring such "internal resonator" effects breaks down above 10% minority concentration. In addition, mode conversion physics must play an increasingly important role at the higher minority concentrations.

INTERNAL TRANSPORT BARRIERS (ITB)

Internal transport barriers have been observed transiently in two types of operation: (i) pellet injection with ICRF minority heating (PEP mode) and (ii) during the majority of H to L mode transitions. Enhanced neutron production is observed in both cases. Off axis RF heating is observed to extend the length of time that the transient neutron production persists in the latter case, possibly through the stabilization of sawteeth. PEP modes at constant plasma currents have been reported as early as 1984 in Alcator-C [19], and 1996 in C-Mod [4,20], whereas PEPs during plasma current ramp, including toroidal rotation measurements were reported only recently [21]. The increase in neutron production at the H to L back transition is also a recent observation [22,23].

In Fig. 13 we show a typical pellet injection shot with ICRF minority heating during plasma current ramp [8], and compare it to PEP during the flat-top current phase. Significant increase in the plasma toroidal rotational speed is also noteworthy during the PEP phase (co-current rotation). We see that during the current ramp ($t = 0.21$ sec) the relative enhancement of the stored energy in the PEP phase is considerably higher than during the flat-top phase ($t = 0.65$ sec). Similarly, the toroidal plasma rotation speed (approaching 80 km/sec at 0.21 sec) is also significantly higher than the 30 km/sec measured at 0.65 sec. However, this latter result could be explained in part by the inverse dependence of the rotation speed on plasma current. It should be noted, however, that while the plasma current increases only by 20% at most, the rotational speed decreases a factor of two when comparing the results at $t = 0.21$ sec and 0.65 sec. We note that the collapse of the PEP at $t = 0.22$ sec coincides with the appearance of sawteeth, whereas the PEP at 0.65 sec collapses well before the occurrence of sawteeth. We also see that the PEP lasts longer during the current ramp (0.15 sec) than during the flat-top phase (0.50 sec). While a possible explanation is the relative timing between pellet injection and ICRF application, another explanation of the better relative results at $t = 0.21$ sec may be a consequence of mildly negative central shear during the current ramp, as may be seen in Fig. 14. The pressure profile has been obtained from kinetic measurements of the density profile and the temperature profile at $t = 0.21$ sec, assuming that $T_e = T_i$ at the high densities, $n_e = 5 \times 10^{20} \mathrm{m}^{-3}$ during the PEP mode. The q_r profile obtained from EFIT [25] reconstruction at $t = 0.21$ sec is also shown, consistent with a mildly reversed profile with $R(q_{min})$ near the half radius (~ 0.78 m), coinciding approximately with the bottom of the steep part of the pressure profile. The width of the shaded curve is indicative of the uncertainties associated with the EFIT reconstruction and includes the possibility that there is no NCS at all. It may be seen that

6

a reasonably well defined ITB is formed at $r/a = 0.5$. Unfortunately, temporal evolution of these profiles has not been obtained to date, but the collapse of the PEP mode coincides with the appearance of sawteeth, presumably due to q_0 decreasing below unity. The collapse of the PEP at 0.65 sec has not been studied, and is not well understood, but the results are typical [4,20]. Future studies will be conducted by maintaining the reversed shear q-profile with off-axis mode-conversion current drive once the new PPPL RF system becomes operational [24]. While the H-factor increases have been modest during the PEP mode phase of the discharge, these results are not very meaningful since the profiles are highly peaked and the shots are in a highly transient state during the evolution of the PEP. In fact, most of the confinement enhancement is in the central part of the plasma volume at radii equal or less than a/2. It has been shown in past experiments that in the central portion of the discharge the average thermal diffusivity approaches the neoclassical value [4].

Results of the enhanced neutron mode (EN mode) are shown in Fig. 15 [22]. Short lived (1 to 3 sawtooth cycles) enhancements in the global neutron production are observed following most H to L mode back transitions in both Ohmic and ICRF heated plasmas [23]. When ICRF heating power is deposited off axis, the sawteeth which typically terminate the mode disappear from the neutron signal. This enables the enhanced neutron rate to persist for a longer period of time. The case shown here resulted when rf power was deposited at $r/a = 0.7$ near the $q = 2$ surface. A minority D(H) heating scenario was used with $B_T = 6.6$ T, Ip=1.0 MA, and $P_{RF} = 2.7$ MW. The density profile in this case has become markedly peaked, and the neutron rate has increased by a factor of 2.5 compared to the level preceding the H to L transition. The ion temperature rises to 2 keV, equivalent to the electron temperature, and is largely responsible for the neutron rate increase. Sawteeth are notably absent from the neutron signal. An analysis of these data indicates [22] that during the enhanced neutron event, the thermal diffusivity in the central portion of the discharge is at or below 0.1 m^2/sec, or an order of magnitude less than typical H-mode values (see Fig. 16). The mode terminates abruptly, perhaps with the onset of MHD activity in the core region.

SUMMARY AND FUTURE DIRECTIONS

In this paper we have shown that ICRF heating in high density, high magnetic field compact tokamak plasmas is very effective. We have investigated minority heating in D(H) and D(^{3}He) scenarios. Typical single pass absorption with the H minority case is of the order of 80-90%, whereas with ^{3}He minority heating it is about 15%. Nevertheless, heating efficiencies of the order of 80-90% have been achieved in both cases. However, with ^{3}He the minority concentration has to be carefully monitored, and for high heating efficiency the concentration has to be kept at 2-3% or mode-conversion heating with possibly lower efficiency may take over. Mode conversion heating and absorption has been explored in

7

different regimes. In general, when the mode conversion layer is located on axis, the absorption efficiency is high (80%). However, when the mode conversion layer is moved off-axis (e.g., $r/a = 0.5$), the absorption efficiency is reduced to $\sim 50\%$. This is lower than full wave codes, such as TORIC would predict, and further work is needed to clarify the situation.

Internal transport barriers (ITBs) have been observed with pellet injection and ICRF minority heating (PEP mode). The persistence of spontaneously occurring ITBs has been lengthened by off axis rf minority heating with reduction of sawtooth activity. These results are transient in nature, namely they last only for 1-2 energy confinement times at most. The reason for this limitation is still not well understood, and remains a challenge for physicists to find means to extend the duration of such high performance modes of operation.

Perhaps the most important new result from C-Mod is the observation of significant toroidal rotation in the co-current direction during RF injection. This rotation is concommitant with observations of increased stored plasma energy, and the effect is particularly strong in the presence of improved confinement, such as H-mode or PEP mode. The very recent observation of significant toroidal rotation in the presence of Ohmic H-mode, without any RF power injection in the plasma, makes the interpretation of these results problematic. In particular, a direct causal relationship between ICRF wave fields and toroidal plasma rotation has not been established.

The ICRF power in C-Mod has been upgraded very recently to 8 MW by the addition of two new transmitters in the frequency range of 40-80 MHz [24]. In addition a new 4-strap antenna has been fabricated by Princeton Plasma Physics Laboratory scientists and installed into C-Mod. The commissioning of this new phaseable antenna has just begun, and should provide exciting new results, including fast wave and mode conversion current drive, shear-flow generation by mode converted IBW, and higher power heating. Of particular importance will be profile control using two different frequencies and heating techniques, as well as combined heating and current drive techniques. It is hoped that some of these techniques will lead to extended high performance modes of operation.

REFERENCES

[1] Porkolab, M. et al, Fusion Energy 1994, (Proc. Fifteenth Int. Conf., IAEA, Seville, Spain, 1993) IAEA-CN-60/A-1-II-2.
[2] Takase, Y., et al., Plasma Physics and Controlled Fusion 38, 2215 (1996).
[3] Takase, Y., et al., Fusion Energy 1996, (IAEA, Vienna, 1, 475 (1997)) IAEA-CN-64/A5-4.
[4] Takase, Y., et al., Phys. Plasmas 4, 1647 (1997).
[5] Bonoli, P. T. et al, Fusion Energy 1996 (IAEA, Vienna, 3, 309, (1997)), IAEA-F1-CN-64/EP-1.

[6] Bonoli, P.T., et al., Phys. Plasmas $\underline{4}$, 1774 (1997).

[7] Takase, Y., et al., Proc. 14th IEEE/NPSS Symp. Fusion Eng., 118, San Diego, CA (1992).

[8] Porkolab, M., et al., Proc. 24th EPS Conf. On Contr. Fusion and Plasma Physics, Berchtesgaden, European Physical Society, Geneva, 21A, II, 569 (1997).

[9] Greenwald, M., et al, Nucl. Fusion $\underline{37}$, 793 (1997).

[10] Greenwald, M., et al., Phys. Plasmas $\underline{6}$, 1943 (1999).

[11] Snipes, J.A., et al, 24th EPS Conf. on Contr. Fusion and Plamsma Physics, Berchtesgaden, EPS, Geneva 21A, II 565 (1997).

[12] Porkolab, M. et al., Plasma Phys. Control. Fusion 40, $\underline{A35}$ (1998).

[13] Rice, J., et al., Nucl. Fusion $\underline{38}$, 75 (1998).

[14] Rice, J., et al., accepted for publication in Nucl. Fusion (1999).

[15] Chang, C.S., Phys. Plasmas, to be published; Fusion Energy to be published, IAEA, Yokohama, Japan, (1998).

[16] Melby, E., et al., Bull. Amer. Phys. Soc, Vol. 45, No. 8 (1998).

[17] Reardon, J., et al, in these Proceedings.

[18] Brambilla, M., Nucl Fusion $\underline{28}$, 549 (1988).

[19] Greenwald, M., et al, Phys. Rev. Lett. $\underline{53}$, 352 (1984); also in Contr. Fusion, IAEA, Kyoto, Vol. I, 139 (1987).

[20] Garnier, D.T., et al., 16th IAEA Fus. Energy Conf., Montreal, (1996), F1-CN-64/AP2-15.

[21] Porkolab, M., Bull. Am. Phys. Soc, Vol. 45, No. 8, 1820 (1998).

[22] Wukitch, S., et al, Bull. Am. Phys. Soc., Vol. 45, No. 8, 1707 (1998).

[23] Fiore, C. et al., Bull. Am. Phys. Soc, Vol. 45, No. 8, 1707 (1998).

[24] Schilling, G. et al., in these Proceedings.

[25] Lao, L.L., et al., Nucl. Fusion $\underline{25}$ 1611 (1985).
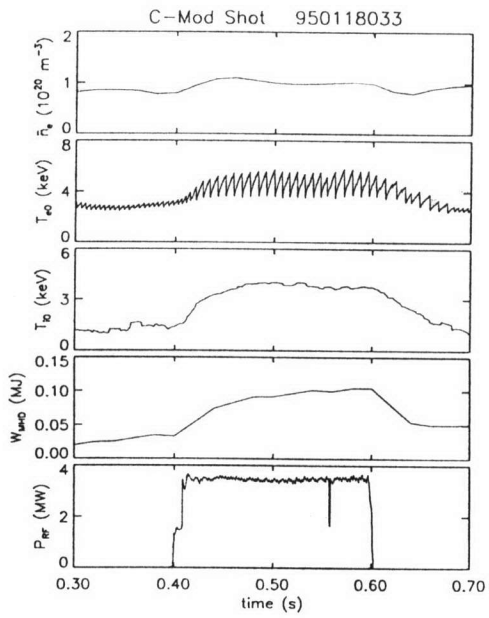
Figure 1: Typical L-mode shot with H-minority at 5.3 T.
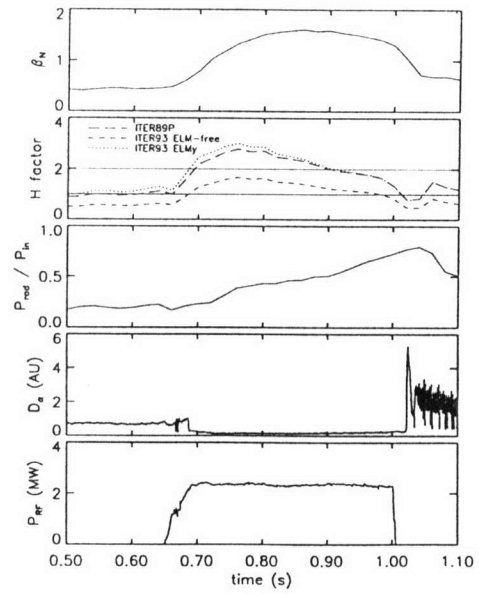
Figure 2: Typical ELM-free H-mode shot at 5.3 T.
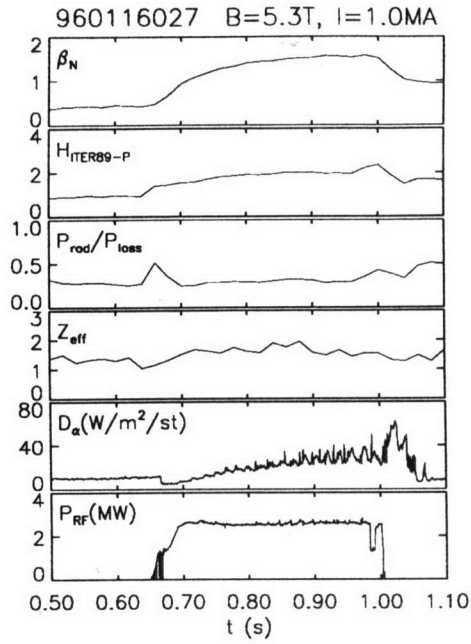
Figure 3: Typical enhanced D_α shot at 5.3 T.
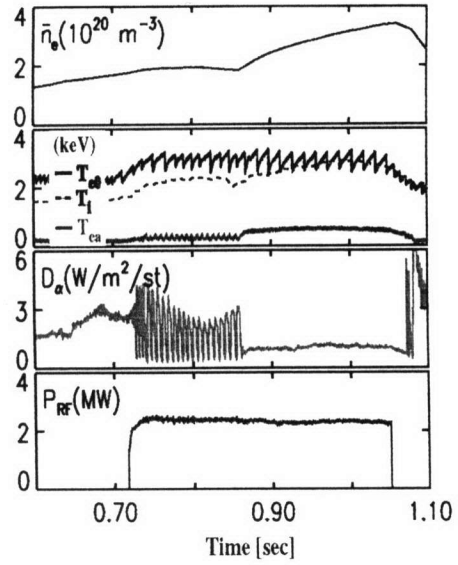
Figure 4: H-Mode transition at 7.9 T with ^{3}He minority species.
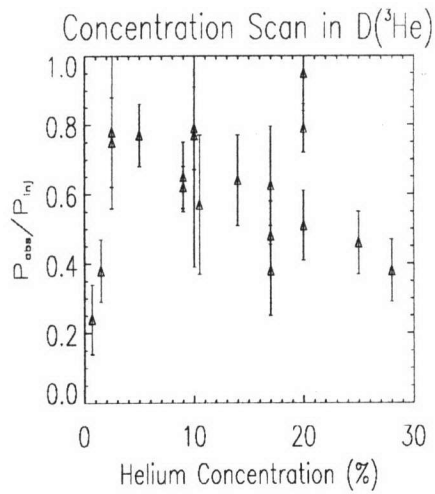

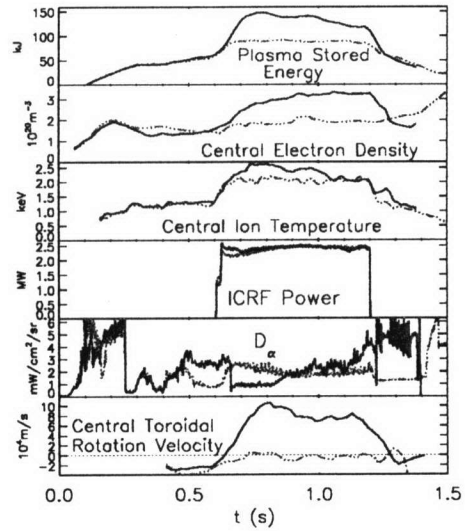Figure 5: RF absorption efficiency vs. ^{3}He concentration in C-Mod at 7.9 T.
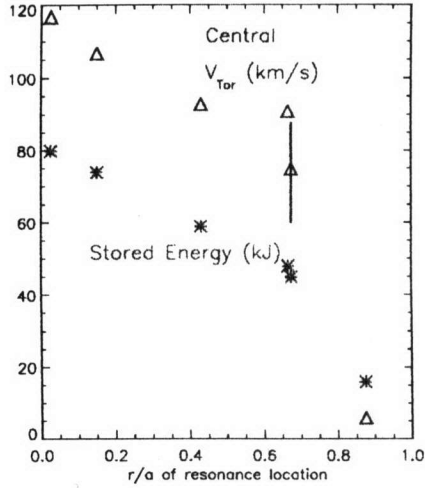

Figure 6 Plasma rotation in L-mode and H-mode at 5.3 T.

Figure 7: Change in stored energy at constant q and toroidal rotation velocity normalized to constant I_p as the resonance location is varied in H-mode plasmas. The toroidal magnetic field is varied to change the resonance location from 5.3 T to 6.9 T.
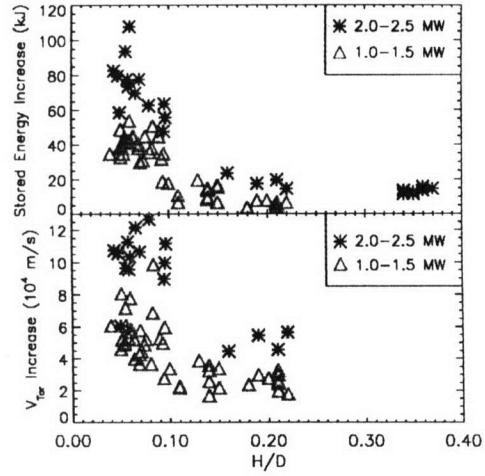
Figure 8: Stored energy (W) and toroidal plasma rotation as the H minority concentration is varied in a D majority plasma at 5.3 T and 0.8 MA. Typical target density is in the range $1.5 - 1.8 \times 10^{20} \mathrm{m}^{-3}$.
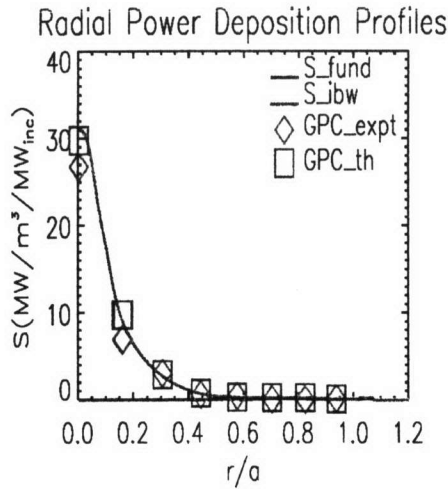
Figure 9: RF power deposition profile by mode conversion at $B = 6.5$ T, $n = 1.5 \times 10^{20} \mathrm{m}^{-3}$, in H majority plasma with 25% ^{3}He minority species.
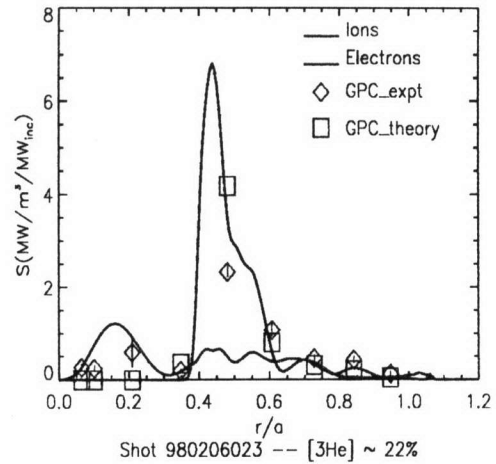
Figure 10: Off-axis RF power deposition profile by mode conversion into IBW at 7.9 T, 1.2 MA and an electron density of $2.5 \times 10^{20} \mathrm{m}^{-3}$ at a ^{3}He minority concentration of 22% in a D-majority plasma.
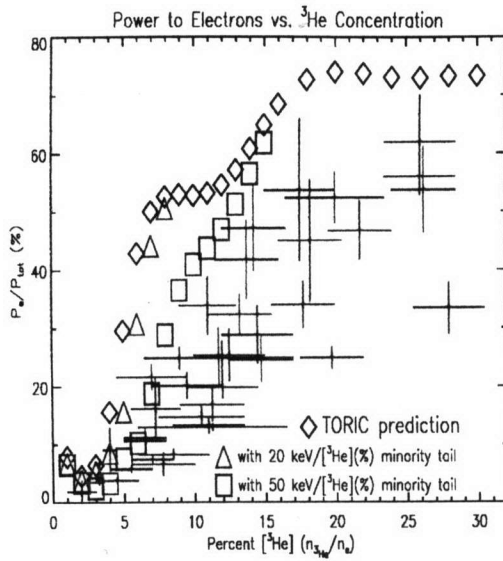
Figure 11: Power absorption by electrons as a function of ^{3}He minority concentration in a D majority plasma. $B = 7.9$ T, 80 MHz. Also shown are the full wave code TORIC predictions.
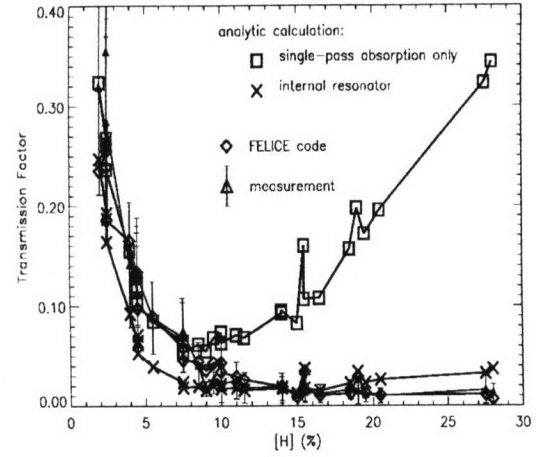

Figure 12: Power transmission versus minority concentration in a D(H) plasma, as determined by magnetic loop probes on the inside wall.
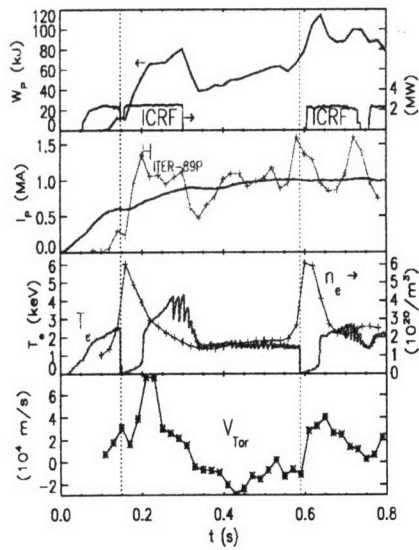

Figure 13: Typical PEP mode shot at $B = 5.3$ T, 80 MHz, H minority heating in D plasma with Li pellet injection.
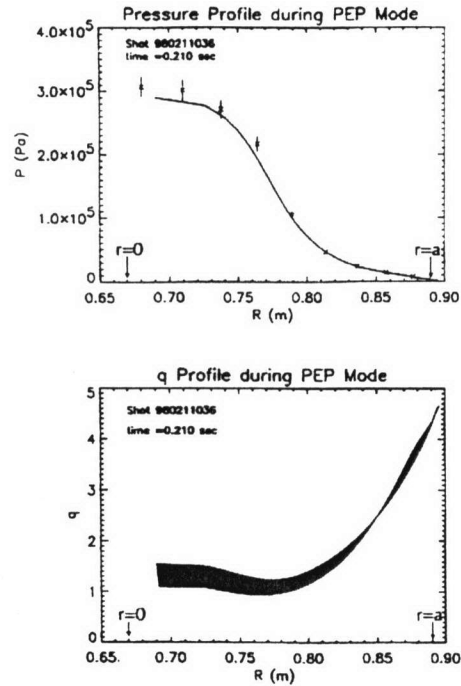

Figure 14: Pressure profile and inferred q profile obtained during the PEP shot of Fig. 13, analyzed at $t = 0.21$ sec.
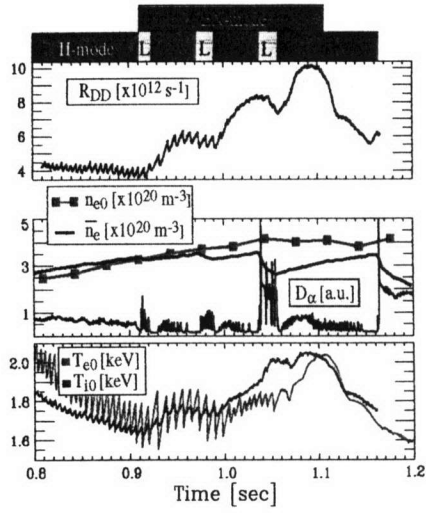
Figure 15: Enhanced neutron mode with off-axis ICRF H-minority heating in a D majority plasma [$B = 6.6$ T, $I_p = 1.0$ MA, $P_{rf} = 2.7$ MW].
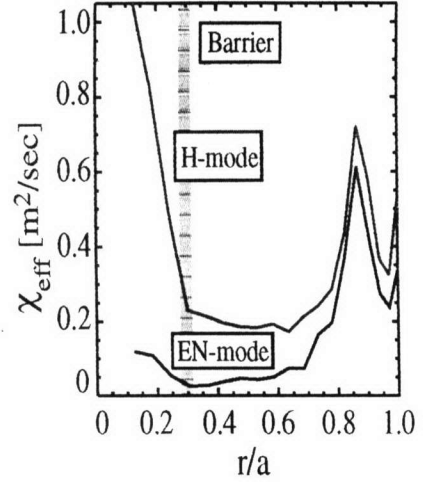

Figure 16: Radial profiles of χ_{eff} corresponding to Fig. 15 during H-mode and the EN-mode.